4652 *Chem. Mater.* **2010,** *22,* 4652–4659
DOI:10.1021/cm100828v

CHEMISTRY OF MATERIALS
Article

Forcing Eu^{3+} into Different Positions in the $BaHfO_3$ Host and Its Spectroscopic Consequences

Anna Dobrowolska and Eugeniusz Zych*

Faculty of Chemistry, University of Wroclaw, 14 F. Joliot-Curie Street, 50-383 Wroclaw, Poland

Received March 23, 2010. Revised Manuscript Received July 12, 2010

Two series of $BaHfO_3$ powders activated with Eu^{3+} ions were prepared with a ceramic method. By stoichiometric variations, the dopant was forced to enter either Ba^{2+} or Hf(IV) sites. X-ray diffraction (XRD) analysis proved that Eu^{3+} ions preferred substitution of Hf(IV) in $BaHfO_3$, while replacement of Ba^{2+} encountered difficulties and led finally to separation of a foreign phase, $Eu_2Hf_2O_7$. Yet, it was shown that the host always incorporated the activator both into Hf(IV) and Ba^{2+} positions, and the two sites, Eu'_{Hf} and $Eu^{\bullet}_{Ba}$, were spectroscopically characterized. From photoluminescence spectra, it appeared that $Eu^{\bullet}_{Ba}$ gave emissions at 573.6, ~595, and 626.0 nm, while luminescence from Eu'_{Hf} was practically limited to just one line peaking at 595.6 nm. Luminescence and excitation spectra taken under synchrotron radiation showed that energy from the excited host is preferentially transferred to Eu'_{Hf} compared to $Eu^{\bullet}_{Ba}$. At 10K, the latter was not capable of intercepting any energy upon excitation above the fundamental absorption of $BaHfO_3$, which limited the luminescence in such conditions to a single line peaking at 595.6 nm. Also, under excitation with X-rays, practically only the Eu'_{Hf} was able to produce luminescence.

Introduction

$BaHfO_3$ activated with Ce^{3+} ions was found to be an attractive scintillator.[1−4] The combination of the high light output of 40 000 ph/MeV[5]), fast decay of the 5d → 4f luminescence of Ce^{3+} ion (25 ns[5]), and high absorption coefficient for X- and γ-rays make this composition a valuable detector even for tools as demanding as positron emission tomography (PET) cameras.[6] Since it is an optically isotropic, cubic (a = 4.171 Å)[7] material, its powders can be compacted and sintered into transparent bodies, whose fabrication is cost attractive compared to making single crystals.[8,9] Some medical diagnostic tools use (or are supposed to use in the future[10]) charge coupled device (CCD) cameras or photodiodes (PD) as electronic detectors of the light emitted by a scintillator. For these devices, having optimal quantum efficiency in the red and near-infrared region of the spectrum, the blue luminescence of $BaHfO_3$/Ce is not that desirable and the fast scintillation flash of Ce^{3+} luminescence is not necessary. Therefore, we decided to activate the $BaHfO_3$ host with Eu^{3+}, whose red luminescence fits much better into the characteristics of CCDs and PDs.[10,11] Our previous scant research showed that Eu^{3+} ions enter the $BaHfO_3$ adopting at least two different symmetries of their surroundings, presumably the sites of Ba^{2+} and Hf(IV).[12] In this paper, we will analyze structural and spectroscopic properties of $BaHfO_3$/Eu phosphors prepared assuming different locations of Eu^{3+} in the host in order to determine the potentiality to force the dopant to substitute just one metal site in the $BaHfO_3$ host, either Ba^{2+} or Hf(IV), and thus to engineer and control the phosphor spectroscopic properties to a higher degree. With such a control, we believe, it might be feasible to turn the $BaHfO_3/Eu^{3+}$ composition into efficient X-ray phosphor. The Kröger-Vink notation of point defects in solids was selected to be used in this paper.[13]

Materials and Methods

Eu-doped barium hafnate compositions were synthesized with a ceramic method using $BaCO_3$ (99.999%), HfO_2 (99.9%), and Eu_2O_3 (99.99%) powders as the starting materials. Three series of compositions were prepared assuming that (a) Eu^{3+} substitutes Hf(IV) ion in the host lattice giving $BaHf_{(1-x)}Eu_xO_3$, Series A;

*To whom correspondence should be addressed. E-mail: zych@wchuwr.pl.

(1) Dole, S. L.; Venkataramani, S. US Patent no. 5124072, 1992.
(2) Venkataramani, V. S.; Loureiro, S. M.; Rane M. V. US Patent no. 6706212 B2, 2004.
(3) Loureiro, M.; Gao, Y.; Venkataramani, V. *J. Am. Ceram. Soc.* **2005**, *88*, 219–221.
(4) Villanueva-Ibañez, M.; Le Luyer, C.; Parola, S.; Dujardin, C.; Mugnier, J. *Opt. Mater.* **2005**, *27*, 1541–1546.
(5) Van Loef, E. V.; Higgins, W. M.; Glodo, J.; Becher, C.; Lempicki, A.; Venkataramani, V.; Moses, W. W.; Derenzo, S. E.; Shah, K. S. *IEEE Trans. Nucl. Sci.* **2007**, *54*(3), 741–743.
(6) Melcher, C. L. *J. Nucl. Med.* **2000**, *41*, 1051–1055.
(7) International Centre for Diffraction Data Database, ICDD, PDF-2 #00-022-0084.
(8) Lempicki, A.; Brecher, C.; Lingertat, H.; Miller, S. R.; Glodo, J.; Sarin, V. K. *Trans. Nucl. Sci. IEEE* **2008**, *55*, 1148–1151.
(9) Jalabadze, N. V.; Chedia, R.; Kukava, T.; Nadaraia, L. *Nucl. Sci. IEEE Trans.* **2008**, *55*, 1514–1522.
(10) Nagarkar, V. V.; Tipnis, S. V.; Miller, S. R.; Lempicki, A.; Brecher, C.; Szupryczynski, P.; Lingertat, H. *Trans. Nucl. Sci. IEEE* **2003**, *50*, 297–300.
(11) Duller, G. A. T.; Bøtter-Jensen, T.; Markey, B. G. *Radiat. Meas.* **1997**, *27*(2), 91–99.
(12) Dobrowolska, A.; Zych, E. Z. Kristallogr. Suppl. 30, **2009**, 367−374, DOI10.1524/zksu.2009.0054.
(13) Nomenclature of Inorganic Chemistry, IUPAC Recommendations 2005, IR-11.4, pp 238−241 (www.iupac.org/publications/books/rbook/Red_Book_2005).

Published on Web 07/27/2010

Table 1. Exemplary Amounts of Starting Materials for Eu Concentratin of 5% for the Three Series

	molar quantity (mmol)		
series	Eu_2O_3	HfO_2	$BaCO_3$
A	0.1267	4.8141	5.0675
B	0.1267	5.0675	4.8141
C	0.1267	4.9408	4.9408

(b) Eu^{3+} substitutes Ba^{2+} ion in the host lattice giving $Ba_{(1-x)}Eu_x$-HfO_3, Series B; (c) Eu^{3+} substitutes Hf(IV) and Ba^{2+} ions in the host lattice with equal probability giving $Ba_{(1-x)}Hf_{(1-x)}Eu_{2x}O_3$, Series C.

The value of "x" varied in the range of 0.005−0.1. In Table 1, exemplary amounts of the starting materials are given for the Eu concentration of 5% for the three series. The substrates were thoroughly mixed and ground in an alumina mortar with acetone as a wetting medium. After drying, the mixture was heated in the air atmosphere at 1400 °C for 4 h. After cooling, the materials were reground and reheated at the same conditions.

Room temperature photoluminescence and excitation spectra were recorded with 0.1 nm resolution using a FSL 920 spectrometer from Edinburgh Instruments. The excitation spectra were recorded with the emission monochromator slits set to 5 nm. A 450 W Xe-lamp was used as an excitation source, and both types of spectra were corrected for the system characteristics. Luminescence decay traces were recorded with the same instrument using its dedicated Xe flash lamp (60 W) as the excitation source. The luminescence and luminescence excitation spectra were also recorded with synchrotron radiation at the Superlumi station of DESY-Hasylab in Hamburg, Germany. The accessible range of wavelengths for excitation was 30−334 nm, and for emission, it was 200−1100 nm. The luminescence was recorded with a CCD camera with resolution of about 0.25 nm. Excitation spectra were corrected for the incident light intensity using sodium salicylate as a standard, and the emissions were corrected for the spectral characteristics of the detection system. The measurements were performed at room temperature (RT) and 10 K. X-ray excited luminescence (XEL) spectra were measured in the range of 200−1100 nm with an Ocean Optics HR2000 CG spectrometer, whose resolution was about 1.2 nm. As the source of excitation, white X-rays from a Cu lamp of a DRON diffractometer were taken and the tube voltage and amperage were 50 kV and 30 mA, respectively. Light output under X-ray stimulation was estimated using a commercial Gd_2O_2S/Eu (GOS/Eu) (Phosphor Technology Ltd., UKL63/F-R1, Dav. $\approx 4\ \mu$m) as a reference material.

The X-ray diffraction (XRD) patterns were measured with a D8 Advance diffractometer (BRUKER) using Cu $K_{\alpha 1}$ radiation ($\lambda = 1.540596$ Å) in the range of $2\theta = 10-120$ degrees with the $\Delta\theta = 0.016°$ step and the counting time of 0.05 s and additionally in the range of $2\theta = 10-70$ degrees with the $\Delta\theta = 0.008°$ step and the counting time of 0.2 s to get a better resolution and signal-to-noise ratio.

Results and Discussion

Powder X-ray Diffraction Analysis. The structural purities of $BaHf_{(1-x)}Eu_xO_3$ (Series A), $Ba_{(1-x)}Eu_xHfO_3$ (Series B), and $Ba_{(1-x)}Hf_{(1-x)}Eu_{2x}O_3$ (Series C) compositions were studied by the powder X-ray diffraction technique. The recorded diffraction patterns are consistent with ICDD card No. 00-022-0084,[7] and results were published elsewhere.[14] They confirm that powders of all three series crystallize in the cubic phase with *Pm*-3 m space group. However, a detailed investigation reveals important and meaningful differences between the three series of Eu-doped $BaHfO_3$ (Figure 1). Namely, especially at higher concentrations of an activator, some cubic-irrelevant reflections of significant intensities appear for powders of Series B and C. The strongest of them are located at 2θ equal to 29.4° and 34.1°. Intensities of the foreign lines are the highest for powders of Series B ($Ba_{(1-x)}Eu_xHfO_3$). In the case of Series C ($Ba_{(1-x)}Hf_{(1-x)}Eu_{2x}O_3$), the cubic $BaHfO_3$ irrelevant lines are less intense, yet they are easily detectable. Only for powders of Series A ($BaHf_{(1-x)}Eu_xO_3$), for which Eu^{3+} ions were forced to replace Hf(IV) in the host, intensities of the extraneous lines are very low even for the highest Eu contents (10%). It is noteworthy that for the most diluted compositions of any series the foreign diffraction lines are practically absent; the discussed effect is clearly dependent on the dopant concentration. The least we can conclude from these results is that the appearance of the foreign phase is facilitated when we force the dopant to substitute Ba^{2+} sites in the host material. Consequently, we deduce that Eu^{3+} prefers substitution of Hf(IV) in $BaHfO_3$, while replacement of Ba^{2+} encounters difficulties and apparently leads to separation of a foreign crystallographic phase.

From the above observations, we infer that the foreign phase separating in powders of Series B and C is related to an Eu−Hf−O composition. Indeed, from the Inorganic Crystal Structure Database[15] as well as published data,[16] $Eu_2Hf_2O_7$ appears to be the most probable compound which separates in materials of Series B and C when heavily doped with Eu. The powders of Series C ($Ba_{(1-x)}Hf_{(1-x)}Eu_{2x}O_3$) were prepared with the premise that two Eu^{3+} ions would enter the host replacing the [Ba^{2+}−Hf(IV)] couple, giving a pair of activators needing no charge compensation. Unfortunately, the results show that even in such circumstances the fraction of the dopant which presumably should replace the Ba^{2+} position in the $BaHfO_3$ host separates, making a new phase. Hence, we deduce that the $BaHfO_3$ lattice without difficulties accepts the Eu^{3+} activator only in the position of Hf(IV). This does not mean that Ba^{2+} is not substituted at all but rather that an achievable concentration of Eu^{3+} ions in this position is expected to be rather minimal. The subsequent spectroscopic results will further confirm these temporary conclusions.

Photoluminescence under UV Excitation. Figure 2 shows emission spectra of $BaHfO_3/Eu^{3+}$ powders of Series A ($BaHf_{(1-x)}Eu_xO_3$, Figure 2a) and B ($Ba_{(1-x)}Eu_xHfO_3$, Figure 2b) recorded upon stimulation into the $O^{2-} \rightarrow Eu^{3+}$ charge transfer (CT) bands located around 260 nm.[12]

(14) Maekawa, T.; Kurosaki, K.; Yamanaka, S. *J. Alloys Compd.* **2006**, *407*, 44–48.

(15) ICSD database, version 1.4.6 (**2009**).

(16) Shlyakhtina Knotko, A. V.; Boguslavskii, M. V.; Stefanovich, S. Yu.; Kolbanev, I. V.; Larina, L. L.; Shcherbakova, L. G. *Solid State Ionics* **2007**, *178*, 59–66.

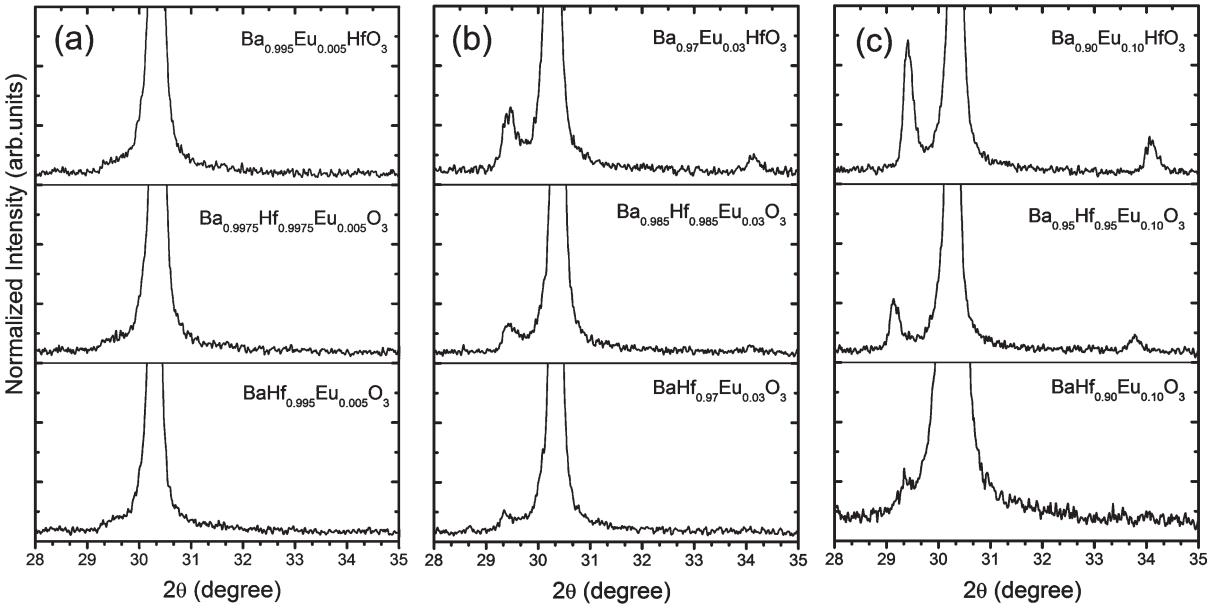

Figure 1. Most significant fragments of XRD patterns for different Eu-activated $BaHfO_3$ compositions with total Eu content equal to (a) 0.5%, (b) 3%, and (c) 10%.

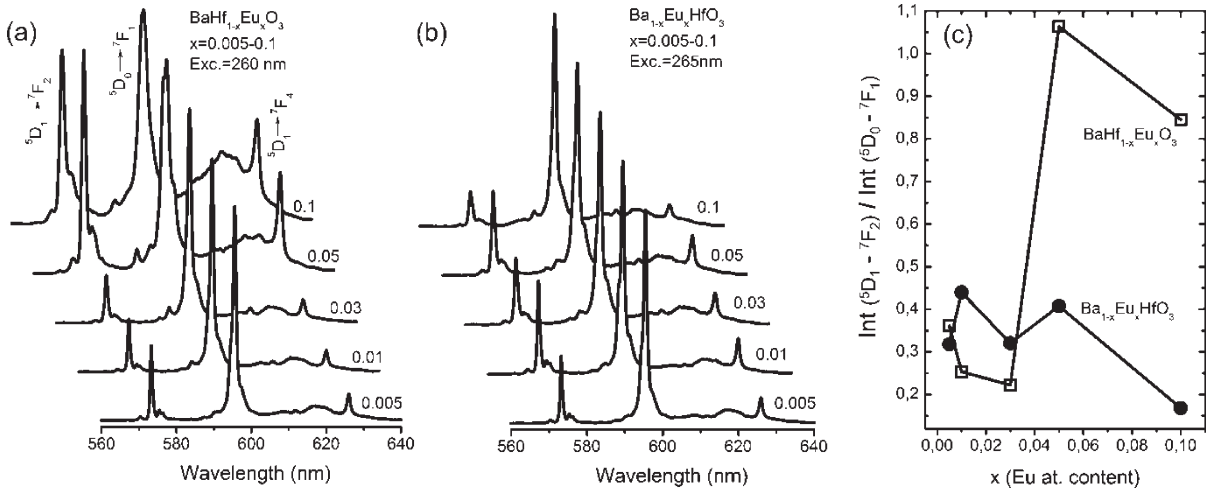

Figure 2. Normalized to the same intensity at 595.6 nm, emission spectra of Eu-activated $BaHfO_3$ powders under excitation into the CT band of Series A ($BaHf_{(1-x)}Eu_xO_3$) (a) and Series B ($Ba_{(1-x)}Eu_xHfO_3$) (b). Variation of the $^5D_1 \rightarrow {}^7F_2/{}^5D_0 \rightarrow {}^7F_1$ emission intensities ratio (c).

Spectra of both series consist of characteristic sharp lines due to the 4f→4f intraconfigurational transitions from the excited $^5D_0$ and $^5D_1$ levels of Eu^{3+} to the components of its ^7F_J states.[17]

The common feature of all spectra is that they consist of two main components, one located at 573.6 nm, resulting from the $^5D_1 \rightarrow {}^7F_2$ radiative relaxation, and another one positioned at 595.6 nm due to the $^5D_0 \rightarrow {}^7F_1$ transition. Both of them are then magnetic dipole induced transitions. The narrow line peaking at 626.0 nm and located at the long-wavelength side of the $^5D_0 \rightarrow {}^7F_2$ component was previously unambiguously proved to result from the $^5D_1 \rightarrow {}^7F_4$ transition as its decay time perfectly matches the one of the $^5D_1 \rightarrow {}^7F_2$ constituent at 573.6 nm.[12] It is characteristic that the electric dipole $^5D_0 \rightarrow {}^7F_2$ emission has a relatively low intensity for any composition, significantly lower than the magnetic dipole induced $^5D_0 \rightarrow {}^7F_1$ one. This is a direct consequence of the metal site symmetries offered by the host lattice. They are presented in Figure 3. It is evident that ligands (O^{2-}) around both Hf(IV) and Ba^{2+} form centrosymmetric environments. Hence, no matter at which metal site the dopant locates, the magnetic-dipole-induced transitions ($\Delta J = 0, \pm 1$, but no $0 \rightarrow 0$ transition) should dominate the spectra[18,19] as long as the necessary charge compensation does not disturb their local symmetries to any significant degree. In fact, it can be taken as a proof that the symmetries around Eu^{3+} ions remain high in the Eu^{3+}-activated $BaHfO_3$.

(17) Karbowiak, M.; Zych, E.; Holsa, J. J. Phys.: Condens. Matter **2003**, 50/YR 15, PII: S0953-8984(03)57449-5, 2169−2181.

(18) Blasse, G.; Grabmeier, B. C. *Luminescent Materials*; Springer−Verlag: New York, 1994.

(19) Shionoya, S.; Yen, W. M. *Phosphors Handbook*; CRC Press LLC: Boca Raton, FL, 1990.

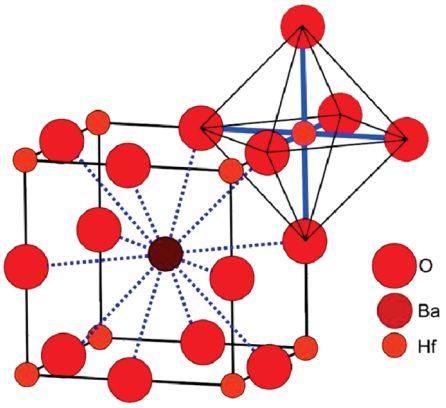

Figure 3. Cubic unit cell of $BaHfO_3$. Ba^{2+} ions are positioned in the center of the cube and surrounded by 12 O^{2-} ions. Hf(IV) ions occupy the corners of the cube and are enclosed by 6 O^{2-} ligands forming an ideal octahedron.

The emission spectra of the two series differ significantly in terms of the variations of the $^5D_1 \rightarrow {}^7F_2/{}^5D_0 \rightarrow {}^7F_1$ transition intensities ratio. In the case of Series A ($BaHf_{(1-x)}Eu_xO_3$, Figure 2a,c), up to the concentration of 3%, the ratio changes only slightly to jump strongly for higher Eu contents. In the range of 5−10%, the intensity of the $^5D_1 \rightarrow {}^7F_2$ (573.6 nm) luminescence matches roughly the strength of the $^5D_0 \rightarrow {}^7F_1$ (595.6 nm) one. Quite a different pattern is observed for the powders of Series B ($Ba_{(1-x)}Eu_xHfO_3$, Figure 2b,c), in which Eu^{3+} was forced to replace Ba^{2+} and for which a separation of a foreign phase in a significant amount was observed using XRD analysis, at least above 1% of Eu concentration (Figure 1). The $^5D_1 \rightarrow {}^7F_2/{}^5D_0 \rightarrow {}^7F_1$ transitions intensities ratio varies only slightly and irregularly within the whole range of Eu contents. These observations, combined with the results of powder diffraction analysis and the results of luminescence kinetics measurements presented below, will allow for further important conclusions to be drawn.

Luminescence Decay Kinetics. Decay traces of the $^5D_1 \rightarrow {}^7F_2$ (573.6 nm) and the $^5D_0 \rightarrow {}^7F_1$ (595.6 nm) emissions were recorded for the powders of Series A and B to further inspect the behavior of the Eu^{3+} dopant ions. The results are presented in Figure 4. A common feature for both series is that the kinetics of the $^5D_1 \rightarrow {}^7F_2$ emission (573.6 nm) is almost independent of the formal Eu concentration. All traces possess a two-exponential character. Yet, with the exception of the systems for which a concentration-related quenching was observed, a dominant component, comprising not less than 80% of the emitted light, could be easily derived in each case. The reason of the appearance of the second, minor constituent is not clear at present. The average decay time constant[20] of the luminescence is about 0.7 ms, and the two components are about 0.4−0.5 ms and 1.8−2.0 ms; quite long for the emission from the $^5D_1$ state. Yet, these values become reasonable when we remember about the high symmetry of the emitting ion environments, for which only the low rate magnetic dipole transitions are allowed.[21] Since for both series of powders, $BaHf_{(1-x)}Eu_xO_3$ (Series A) and $Ba_{(1-x)}Eu_xHfO_3$ (Series B), the speed of the $^5D_1 \rightarrow {}^7F_2$ (573.6 nm) luminescence decay is so akin, we anticipate that the emitting centers producing it should be of the same type in each case.

Importantly, in general, the emission from the $^5D_1$ level is prone to quenching[18,22] and is hardly observed at room temperature, especially at higher concentrations of the Eu^{3+}.[18] In the investigated powders, the decay time of the state is practically independent of the formal Eu concentration. This may be taken as an indication that the population of the emitting center producing this luminescence is in fact low and remains roughly constant in all samples, despite formally the concentration increases by a factor of 20. The situation is much different in the case of the $^5D_0 \rightarrow {}^7F_1$ emission whose main component peaks at 595.6 nm. For the powders of Series B ($Ba_{(1-x)}Eu_xHfO_3$), this luminescence is only slightly quenched for the highest concentrations. A totally different pattern is seen for this emission in the case of powders of Series A ($BaHf_{(1-x)}Eu_xO_3$), for which an increasing quenching appears when the Eu content exceeds 3%. The average decay time constant of this component drops from 4.2 ms (0.5%) to 2.0 ms (10%). Let us note that this effect perfectly mirrors the variations in the $^5D_1 \rightarrow {}^7F_2/{}^5D_0 \rightarrow {}^7F_1$ transition intensities ratio presented in Figure 2c. Consequently, we conclude that the relative increase of the intensity of the $^5D_1 \rightarrow {}^7F_2$ luminescence in the powders of Series A above 3% of the Eu content is in fact caused by the quenching of the $^5D_0 \rightarrow {}^7F_1$ emission at 595.6 nm. Results presented in Figures 2 and 4 utterly support each other and apparently explain the concentration-induced differences in the emission spectra of both series.

The results of kinetics measurements remain also in an agreement with the conclusions drawn from XRD analysis. Since for Series B ($Ba_{(1-x)}Eu_xHfO_3$) a significant (and increasing with concentration) fraction of Eu was found to separate as $Eu_2Hf_2O_7$, only the remaining small portion of the activator entered the $BaHfO_3$ host. Consequently, the genuine content of the dopant in the barium hafnate lattice remained low and approximately constant despite increasing formal concentration, exactly as concluded from the luminescence decay measurements.

Yet, decay kinetics allow for further conclusions to be derived. Since for the Series A ($BaHf_{(1-x)}Eu_xO_3$) the lower-energy $^5D_0 \rightarrow {}^7F_1$ luminescence experiences a significant shortening of its duration above the concentration of 3% and simultaneously the higher-energy $^5D_1 \rightarrow {}^7F_2$ emission is practically not quenched at all, we deduce that the 573.6 and 595.6 nm features result from processes occurring within different Eu^{3+} ions. From this, an obvious supposition appears that one of the emissions results from Eu^{3+} occupying the position of Ba^{2+} and another one from the activator which replaced Hf(IV).

(20) Berberan-Santos, M. N.; Bodunov, E. N.; Valeur, B. *Chem. Phys.* **2005**, *317*, 57–62.
(21) Zych, E. *J.Phys.: Condens. Mater* **2002**, *14*, 5637–5650.
(22) Blasse, G. *Mater. Chem. Phys.* **1987**, 16201–236.

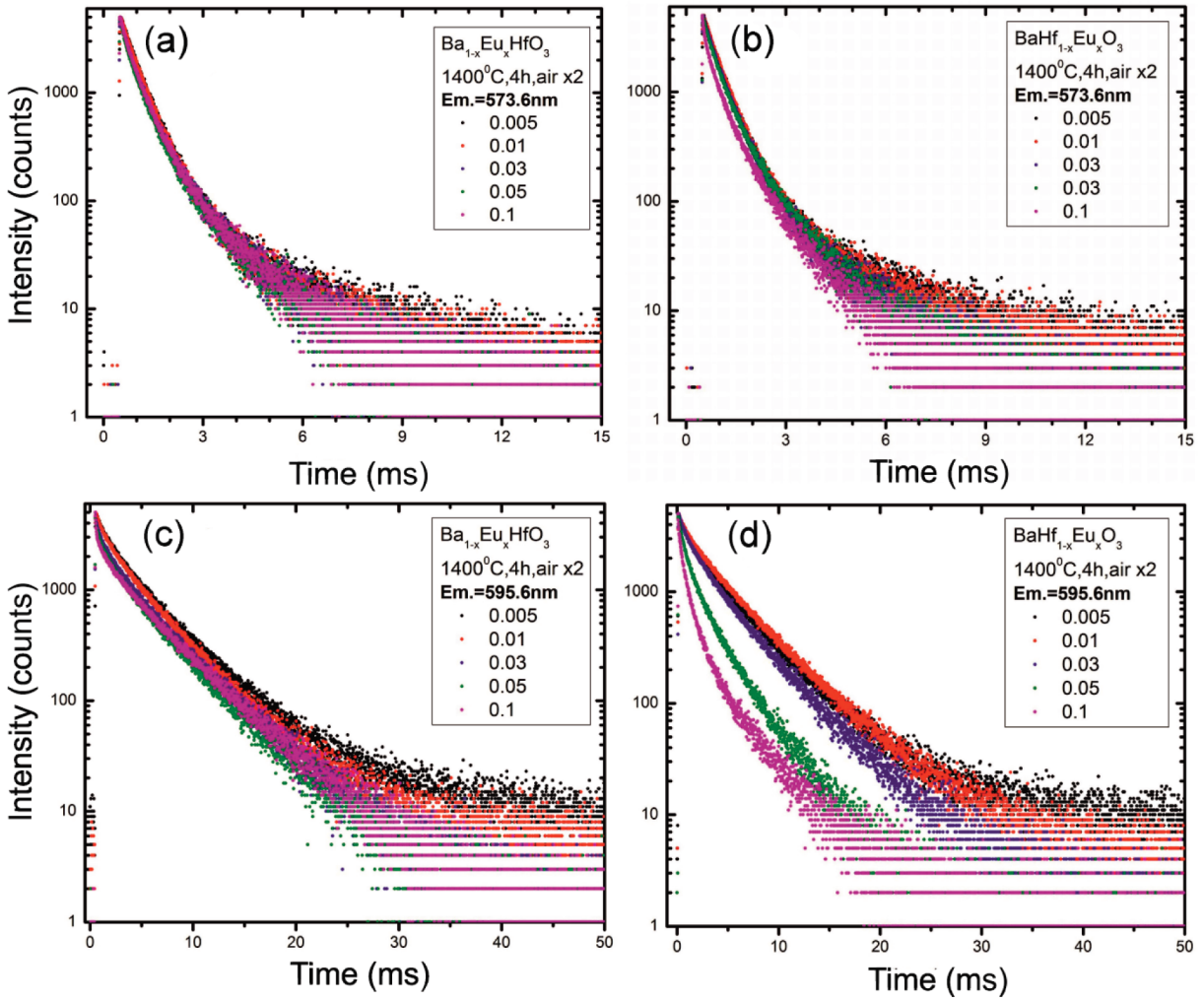

Figure 4. Decay traces of the main luminescences in different compositions of Eu-doped $BaHfO_3$ (a−d).

We have already shown above that Eu^{3+} can hardly replace Ba^{2+} but is quite eager to substitute Hf(IV) even at higher concentrations. Hence, Eu^{3+} in the position of the former cannot attain any higher population. Consequently, we may expect that emission of these ions will not be prone to quenching.

However, since Eu^{3+} forced to substitute the site of Hf(IV) (as in the Series A) can indeed achieve high concentrations, its luminescence may be subjected to quenching after its content prevails over a critical value. Our results showed that the critical concentration was 3% (Figure 4). Then, it appears that the 573.6 nm emission related to the $^5D_1 \rightarrow {}^7F_2$ transition results from the small fraction of Eu^{3+} ions occupying the position of the Ba^{2+} site, while the 595.6 luminescence occurs due to Eu^{3+} ions in the Hf(IV) location. Yet, we can further precise this general conclusion taking into account the results of the site selective spectroscopy presented already in our previous report.[12] Namely, it appears that the Eu^{3+} in the Ba^{2+} position produces also some emission in the range of 592−600 nm, exactly where the Eu^{3+} in Hf(IV) gives its predominant luminescence (595.6 nm). Thus, now, we are in the position to state that the $Eu^{\bullet}_{Ba}$ ions produce the 573.6 and 626.0 nm emissions as well as some luminescence around 595.6 nm, while Eu'_{Hf} gives almost exclusive emission at 595.6 nm.

Let us yet note that also the decay time of the 595.6 nm emission in the diluted compositions are relatively long (4.2 ms). This again proves that the symmetry around Eu^{3+} ions does not get any significant distortion as only in a centrosymmetric environment such long decay times can occur for Eu^{3+} ions. Hence, for low concentration systems, the compensation of the different charge of Eu^{3+} has to rarely take place in its direct vicinity.

Spectroscopy under Excitation with UV-VUV and X-rays. Figure 5 presents, normalized at 595.6 nm, XEL spectra of the powders of Series A ($BaHf_{(1-x)}Eu_xO_3$, Figure 5a) and Series B ($Ba_{(1-x)}Eu_xHfO_3$, Figure 5b). No XEL emission was observed outside the presented region of 550−650 nm. At present, the light yield for the best sample does not exceed 10% of that produced by commercial GOS/Eu.[23] Compared to the already presented photoluminescence (PL) emissions, the most distinctive feature of the XEL spectra is their much less complex structure. All of

(23) Michail, C. M.; Valais, I. G.; Toutountzis, A. E.; Kalyvas, N. E.; Fountos, G. P.; David, S. L.; Kandarakis, I. S.; Panayiotakis, G. S. *Trans. Nucl. Sci. IEEE* **2009**, *55*, 3703–3709.

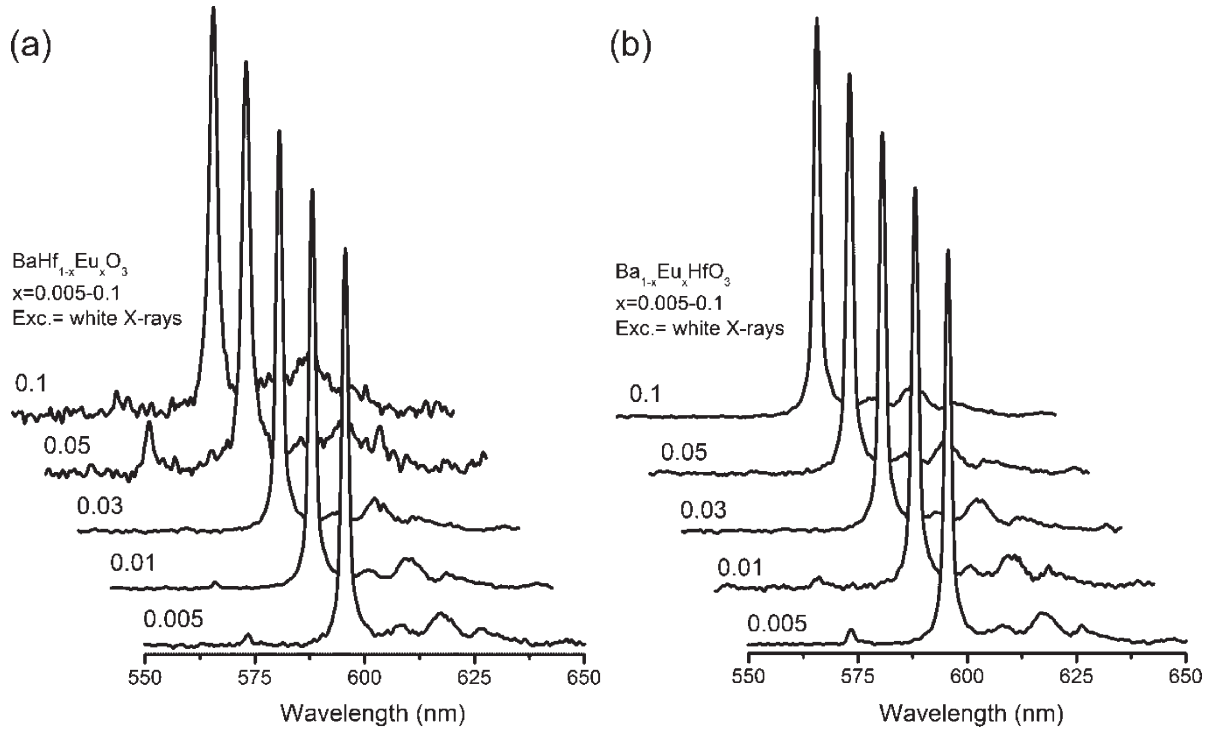

Figure 5. XEL spectra of Series A ($BaHf_{(1-x)}Eu_xO_3$) (a) and Series B ($Ba_{(1-x)}Eu_xHfO_3$) (b). All spectra were normalized at their maxima at 595.6 nm.

them are dominated by the line peaking at 595.6 nm, which was earlier attributed to the $^5D_0 \rightarrow {}^7F_1$ transition of the Eu^{3+} ion located in the Hf(IV) site. In XEL spectra, the luminescence from $^5D_1$ level, in PL seen at 573.6 nm ($^5D_1 \rightarrow {}^7F_2$) and at 626.0 nm ($^5D_1 \rightarrow {}^7F_4$), produces only residual insignificant structures or, more often, does not come into view at all. According to the earlier analysis, we take it as an indication that $Eu^{\bullet}_{Ba}$ ions are basically inactive in producing luminescence under X-ray stimulation. Synchrotron radiation measurements in the vicinity of the band gap energy shed more light on that surprising difference between PL and XEL.

Figure 6 compares room temperature (RT) excitation spectra of the lightly doped (0.5%) powders of Series A (Figure 6a) and Series B (Figure 6b). Reflectance spectra of both materials are also included. From the latter, the absorption edge of the host materials can be positioned around 225 nm at RT. Above that value (at longer wavelengths), broad structured excitation bands are seen for both 573.6 and 595.6 nm emissions for materials of each series. However, only in the excitation spectrum of the 595.6 nm luminescence, a significant rise of the efficiency is observed around 229 nm, just in the direct proximity of the band gap absorption. Calculated differential excitation spectra of the 595.6 and 573.6 nm emissions of both powders, $BaHf_{(1-x)}Eu_xO_3$ (Series A) and $Ba_{(1-x)}Eu_xHfO_3$ (Series B), are presented in Figure 6c,d, respectively. In both cases, a well-defined, quite narrow line peaking at 229 nm is seen. This position is 0.1 eV below the band gap energy (225 nm). From these observations, we can reasonably ascribe the 229 nm component appearing basically only in the excitation spectrum of the 595.6 nm luminescence to a free exciton formation. This further implies that the excitonic energy is more efficiently transferred to the Eu^{3+} ions in the (negatively charged) Eu'_{Hf} sites and produces the luminescence at 595.6 nm compared to the dopant in the (positively charged) $Eu^{\bullet}_{Ba}$ sites which chiefly sends off the photons of 573.6 nm.

Luminescence spectra recorded under stimulation with synchrotron radiation at 80 nm (host fundamental absorption) and 260 nm (CT excitation), presented in Figure 7, further support these conclusions. These spectra are practically identical for all series. Those in Figure 7 come from the 0.5% sample of Series B. At room temperature, emissions under 80 and 260 nm differ to some extent but not significantly. Yet, the 573.6 nm luminescence intensity relative to the 595.6 nm one is significantly lower under 80 nm stimulation. The 595.6 nm emission is also slightly narrower. Both these subtle differences become much more meaningful after reducing the sample temperature to 10 K. Then, the energy of 80 nm radiation absorbed by the host does not transfer into any luminescence at 573.6 nm, hence from the $Eu^{\bullet}_{Ba}$ site.

Instead, only a narrow line peaking at 595.6 nm of the Eu'_{Hf} comes into view. In contrary, the 260 nm radiation, which excites directly the dopant, leads to both the 573.6 and 595.6 nm emissions. At 10 K, the latter luminescence is also much broader than its counterpart produced with 80 nm radiation. This effect results from the fact that around 595 nm also the $Eu^{\bullet}_{Ba}$ produces some emission with components spreading over the 592−600 nm region.[12] The 80 nm excitation simulates to some extent stimulation with X-rays, as it also excites the $BaHfO_3$ host. Thus, the low temperature additionally reduces the relative efficacy of the energy transfer from the host material to $Eu^{\bullet}_{Ba}$ compared to Eu'_{Hf}. Hence, all observations prove that the excited host prefers passing its excessive energy to Eu'_{Hf} rather than to $Eu^{\bullet}_{Ba}$. In fact,

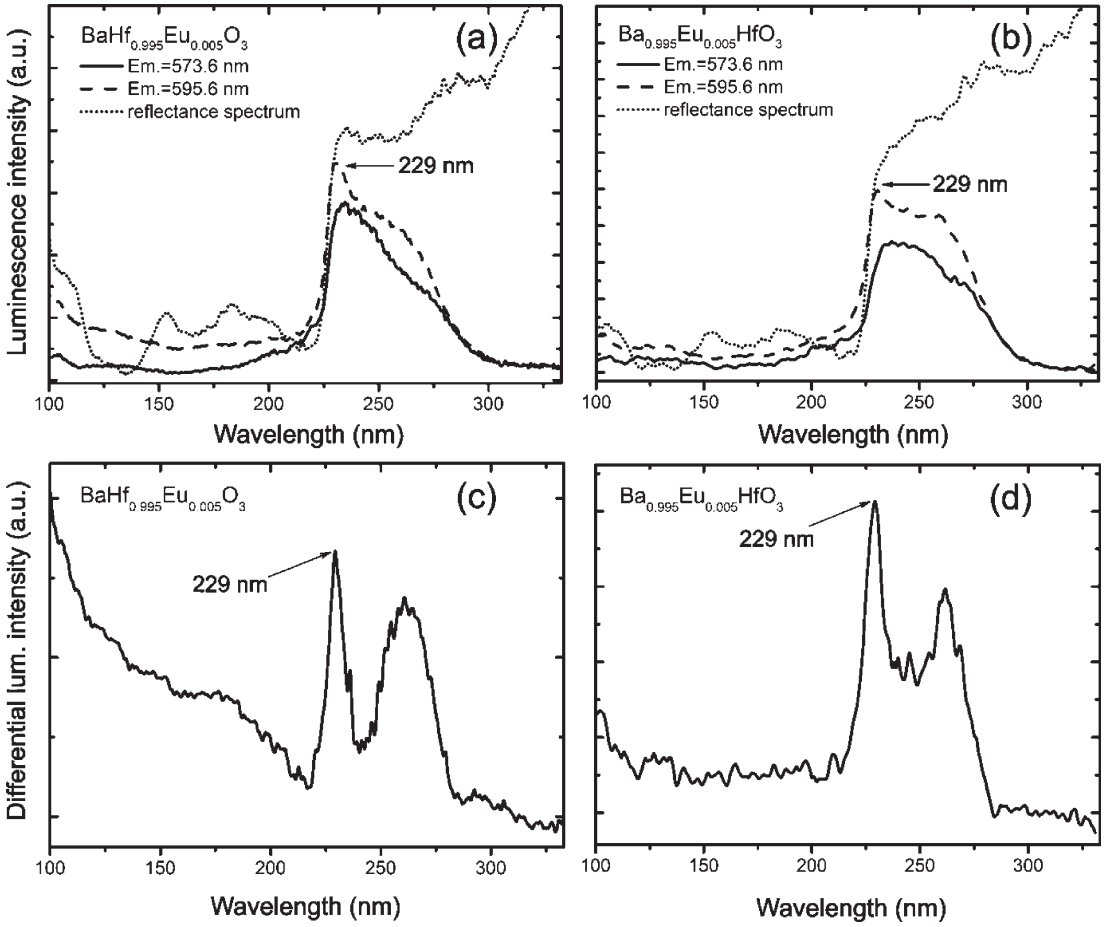

Figure 6. Room temperature luminescence excitation and reflectance spectra of powders of Series A (a) and Series B (b) containing 0.5% of the dopant. Calculated differential excitation spectra of emissions located at 595.6 and 573.6 nm for Series A (c) and Series B (d). The narrow line peaking at 229 nm is ascribed to free exciton formation.

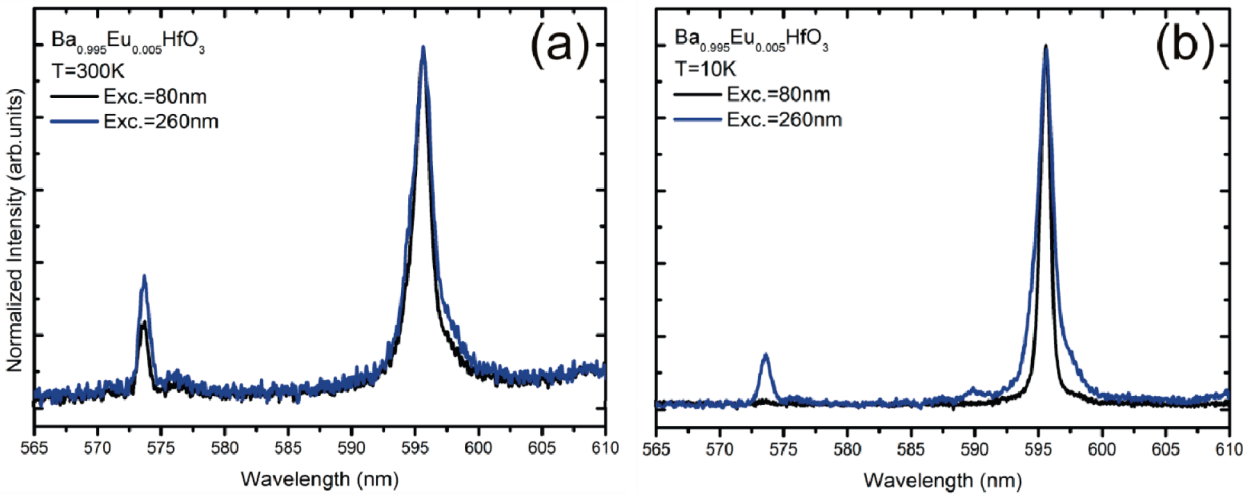

Figure 7. Luminescence spectra of $Ba_{0.995}Eu_{0.005}HfO_3$ powder recorded under excitation at 80 and 260 nm with synchrotron radiation at RT (a) and 10 K (b).

some indication of that difference in intercepting the energy from the host by the two Eu ions could be already noted in the excitation spectra on Figure 6 a,b. The signals below 225 nm are very low for materials of each series which also elucidates why the XEL emissions are inefficient. Yet, the excitation of the 595.6 nm luminescence in the short-wavelengths region is clearly more efficient compared to excitation of the 573.6 nm emission. This indicates that the energy acquired by the host and stored in free carriers, though generally inefficiently, is being transferred preferentially to Eu'_{Hf} ions producing the luminescence at 595.6 nm.

Wojtowicz evidenced that at first Eu^{3+} ions preferentially intercept holes becoming Eu^{2+}, and only afterward,

interception of electrons revert the dopant to the Eu^{3+} already in an excited state.[24] This stays in agreement with our findings as the interception of a hole is obviously more probable by Eu^{3+} ions in Eu'_{Hf} sites with a negative net charge than in $Eu^{\bullet}_{Ba}$, whose positive net charge generates an extra barrier for that process making it inefficient. As it was discussed above, also, excitons transfer their excessive energy to the Eu'_{Hf} sites more efficiently than to $Eu^{\bullet}_{Ba}$. There may be a mutual reason of both effects. If the very bottom of the conduction band consists of basically Hf(IV) (empty) states, which is reasonable due to its higher electronegativity compared to Ba, then the thermalized electrons, either free or bound into excitons, diffuse from the position of their creation to the activator through the oxygen−hafnium sublattice. Consequently, the probability they will dissipate their energy at Eu'_{Hf} sites becomes naturally higher. In such a way, all the experimental findings create a consistent picture with the remaining problem being whether or not it is possible to improve the efficiency of XEL of $BaHfO_3$ activated with Eu^{3+} ions.

(24) Wojtowicz, A. J. In *Proceedings of the International Conference on Inorganic Scintillators and their Applications SCINT95*; Dorenbos, P.; Van Eijk, C. W. E., Eds.; Delft University Press: Delft, The Netherlands, 1996; pp 95−102.

Conclusions

Eu^{3+} activated $BaHfO_3$ powders were prepared with a ceramic method at 1400 °C, forcing the dopant by stoichiometry to replace either Ba^{2+} or Hf(IV). $BaHf_{(1-x)}Eu_xO_3$ powders are crystallographically pure, while in the $Ba_{(1-x)}Eu_xHfO_3$ series, the dopant separated as $Eu_2Hf_2O_7$ when its content exceeded 1%. Independently, on the stoichiometry, the host incorporated the activator both into Ba^{2+} and Hf(IV) positions. Only in the $BaHf_{(1-x)}Eu_xO_3$ series, a significant quenching of the emission from Eu'_{Hf} ions was found. PL and XEL spectra differed significantly, with the latter being less complex and lacking the high energy portion of the emission compared to the former. High energy synchrotron excitation revealed that excitons as well as free carriers transferred their energy to the Eu'_{Hf} sites preferentially compared to $Eu^{\bullet}_{Ba}$. This effect became even more profound at low temperatures, when stimulation with 80 nm radiation did not produce any luminescence from $Eu^{\bullet}_{Ba}$ sites.

Acknowledgment. The research was supported by EU Program of Innovative Economy POIG.01.01.02-02-006/09 and under the DESY HasyLab Grant #II-20090289 EC. A. D. acknowledges the support of Marshal Council of Lower Silesia and EU for *GRANT-Supporting Research through Scholarships for Doctoral Students*.